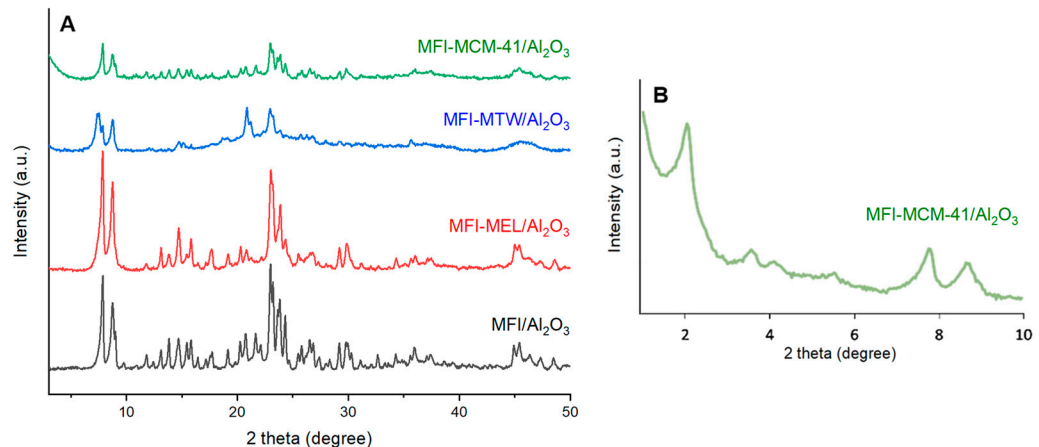


## Supplementary Materials

**Table S1.** Composition of hybrid zeolites [15].

	Phase ratio	Si/Al, mol/mol
MFI-MEL	55 (MFI):45 (MEL)	53
MFI-MTW	60 (MFI):40 (MTW)	53
MFI-MCM-41	80 (MFI):20 (MCM-41)	55
MFI	100 (MFI)	48



**Figure S1.** XRD patterns of the catalysts. **(A)** WAXRD-patterns **(B)** SAXRD-pattern of MFI-MCM-41/Al<sub>2</sub>O<sub>3</sub> [15].

**Figure S1:** According to XRD patterns of the catalysts, all samples contain the MFI topology structure, as evidenced by the presence of specific to MFI reflections at  $2\theta = 7.9$ ,  $8$ ,  $23.2$ ,  $23.9$ , and  $24.4^\circ$ .

The presence of the MEL structure in the MFI-MEL/Al<sub>2</sub>O<sub>3</sub> sample is confirmed by the presence of reflections at  $2\theta = 7.92$ ,  $8.78$ ,  $23.14$ ,  $23.98$  and  $45.2^\circ$ . The MFI-MTW/Al<sub>2</sub>O<sub>3</sub> catalyst XRD pattern contains reflections that are characteristic of the MTW type structure at  $2\theta = 7.2$ ,  $8.8$ ,  $20.7$ , and  $23.1^\circ$ . The presence of MCM-41 in the MFI-MCM-41/Al<sub>2</sub>O<sub>3</sub> catalyst is confirmed by the characteristic reflection of the amorphous SiO<sub>2</sub> of MCM-41 at  $2\theta = 22.8^\circ$  and the reflection at  $2\theta = 2.2^\circ$  on small-angle X-ray diffraction pattern [15].

**Table S2.** Textural properties of the catalysts [15].

	MFI-MEL/Al <sub>2</sub> O <sub>3</sub>	MFI-MTW/Al <sub>2</sub> O <sub>3</sub>	MFI-MCM-41/Al <sub>2</sub> O <sub>3</sub>	MFI/Al <sub>2</sub> O <sub>3</sub>
Total	0.286	0.443	0.340	0.198
V(pore), cm <sup>3</sup> /g(cat)	Micro 0.088 (30.8%) Meso 0.198 (69.2%)	0.012 (2.7%) 0.431 (97.3%)	0.040 (11.8%) 0.300 (88.2%)	0.057 (28.7%) 0.142 (71.3%)
S <sub>BET</sub> , m <sup>2</sup> /g(cat)	361	179	250	293
S <sub>micro</sub> , m <sup>2</sup> /g(cat)	250	11	42	181
S <sub>meso</sub> , m <sup>2</sup> /g(cat)	95	101	185	96
S <sub>external</sub> , m <sup>2</sup> /g(cat)	15	67	24	14
d <sub>micro</sub> <sup>1</sup> , nm	0.91	0.69	0.63	0.90
d <sub>meso</sub> <sup>2</sup> , nm	5.79	19.67	7.58	8.27
IHF <sup>3</sup>	0.51	0.07	0.45	0.34

<sup>1</sup>average micropore diameter (MP-plot)

<sup>2</sup>average mesopore diameter (BJH method)

<sup>3</sup>IHF – indexed hierarchy factor of the catalysts [22]

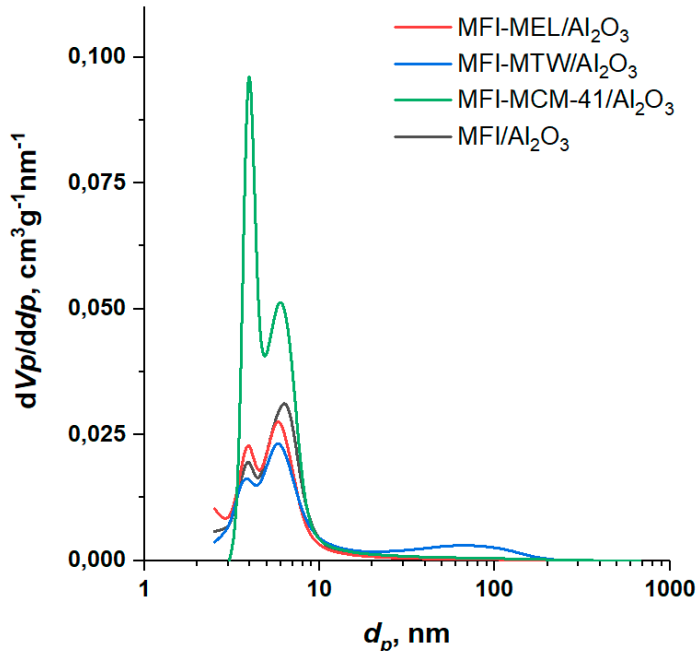


**Figure S2.** BJH plots (desorption curve) for the catalysts MFI-MEL/Al<sub>2</sub>O<sub>3</sub>, MFI-MTW/Al<sub>2</sub>O<sub>3</sub>, MFI-MCM-41/Al<sub>2</sub>O<sub>3</sub>, and MFI/Al<sub>2</sub>O<sub>3</sub> [15].

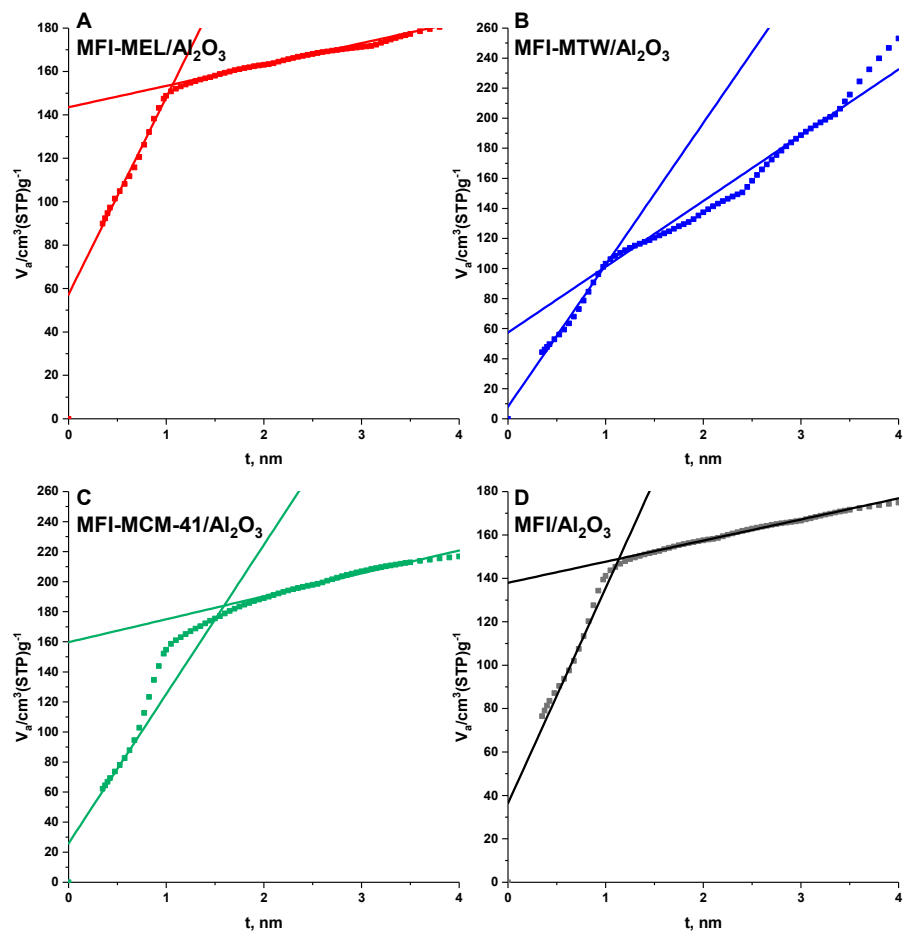


**Figure S3.** t-plots for nitrogen adsorbed in the catalysts MFI-MEL/Al<sub>2</sub>O<sub>3</sub> (**A**), MFI-MTW/Al<sub>2</sub>O<sub>3</sub> (**B**), MFI-MCM-41/Al<sub>2</sub>O<sub>3</sub> (**C**), and MFI/Al<sub>2</sub>O<sub>3</sub> (**D**) [15].

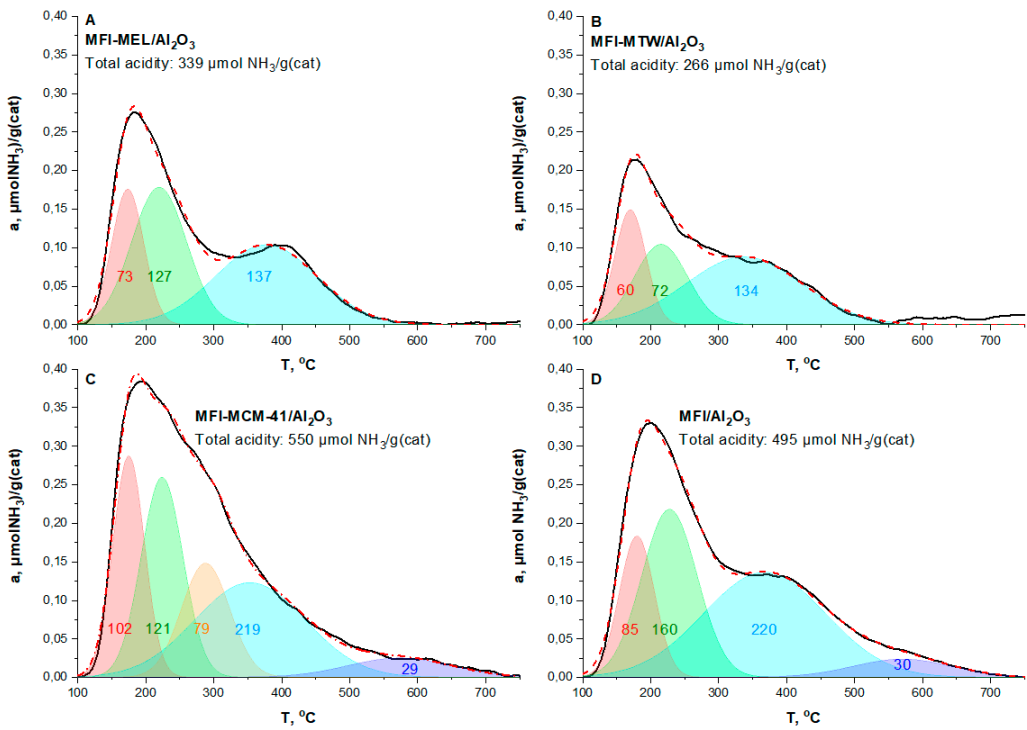


**Figure S4.** NH<sub>3</sub>-TPD profiles of ammonia (A) MFI-MEL/Al<sub>2</sub>O<sub>3</sub>, (B) MFI-MTW/Al<sub>2</sub>O<sub>3</sub>, (C) MFI-MCM-41/Al<sub>2</sub>O<sub>3</sub>, (D) MFI/Al<sub>2</sub>O<sub>3</sub> and their deconvolution into Gaussian peaks. The black solid line is the experimental curve. The red dotted line is the cumulative curve of Gaussian peaks. Numbers indicate the amount of acid sites corresponding to the peak,  $\mu\text{mol NH}_3/\text{g(cat)}$  [15].

**Table S3.** Acidic properties of catalysts [15].

№	Sample	Acidity of Fresh Catalyst, $\mu\text{mol NH}_3/\text{g (cat)}$					
		Total	Weak Sites		Medium Sites		
			$T_1 = 170 - 180 \text{ } ^{\circ}\text{C}$	$T_2 = 215 - 230 \text{ } ^{\circ}\text{C}$	$T_3 = 290 \text{ } ^{\circ}\text{C}$	$T_4 = 350 - 380 \text{ } ^{\circ}\text{C}$	
1	MFI-MEL/Al <sub>2</sub> O <sub>3</sub>	339	200 (59.0 %)		-	139 (41.0 %)	-
2	MFI-MTW/ Al <sub>2</sub> O <sub>3</sub>	266	132 (49.6%)		-	134 (50.4 %)	-
3	MFI-MCM-41/ Al <sub>2</sub> O <sub>3</sub>	550	223 (40.5 %)	79 (14.4 %)	219 (39.8 %)	29 (5.3 %)	
4	MFI/Al <sub>2</sub> O <sub>3</sub>	495	245 (49.5 %)		-	220 (44.4 %)	30 (6.0 %)

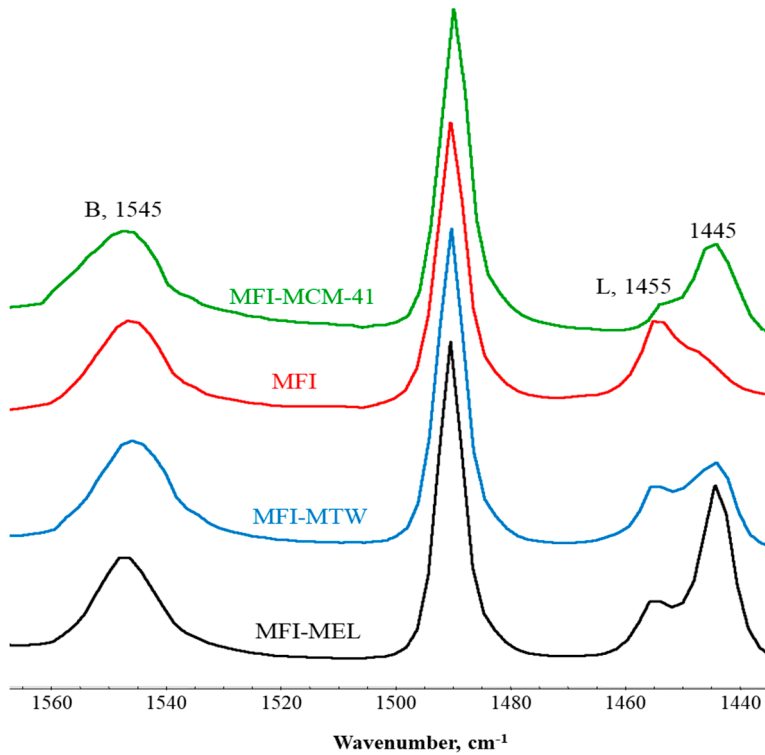


**Figure S5.** IR spectra of pyridine adsorbed on hybrid zeolites [15].

**Figure S5:** For all samples in the IR spectra of absorbed pyridine, the peaks at  $1455\text{ cm}^{-1}$  and  $1545\text{ cm}^{-1}$  indicate the adsorption of pyridine on strong Lewis and Brønsted acid sites, respectively. The peak at  $1445\text{ cm}^{-1}$  characterizes physically adsorbed pyridine [15].

**Table S4.** Acid characteristics of hybrid zeolites [15].

	Number of acid sites, $\mu\text{mol Py/g}$			$B/L$
	<i>BASs</i>	<i>LAs</i> s	<i>Total</i>	
MFI-MEL	90	25	115	3.6
MFI-MTW	110	27	137	4.1
MFI-MCM-41	85	20	105	4.3
MFI	80	35	115	2.3

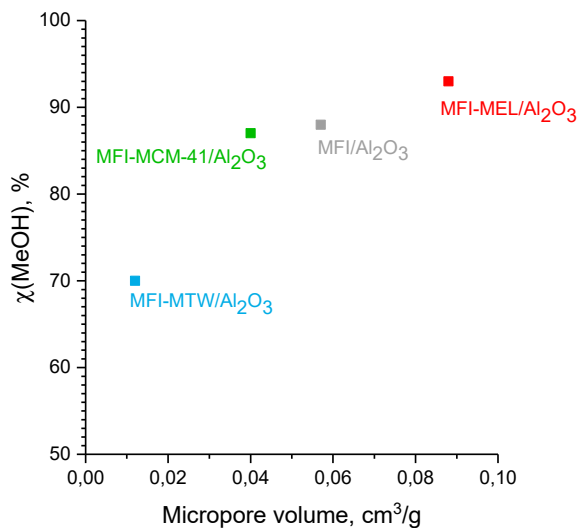


**Figure S6.** Dependence of methanol conversion on the volume of micropores in the catalyst. T = 340°C, P = 10.0 MPa.  $\tau = 0.6 \text{ h}^*\text{g(C)/g(cat)}$ .

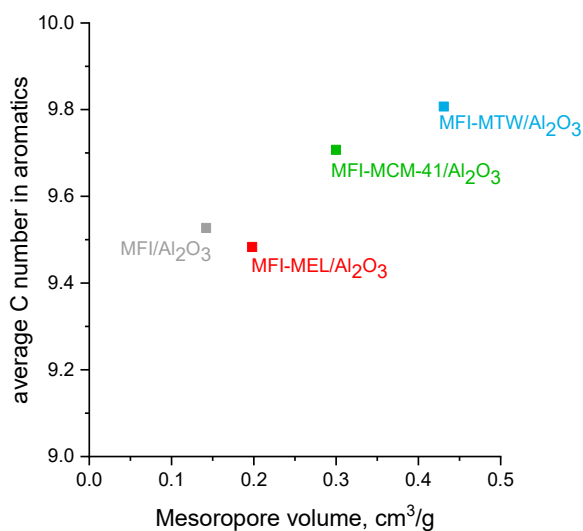


**Figure S7.** Dependence of average number of carbon atoms in aromatic compounds on the volume of mesopores in the catalyst. T = 340°C, P = 10.0 MPa.  $\tau = 0.6 \text{ h}^*\text{g(C)/g(cat)}$ .

## References

15. Magomedova, M.V.; Starozhitkaya, A.V.; Davidov, I.A.; Tsaplin, D.E.; Maximov, A.L. Dimethyl Ether to Olefins on Hybrid Intergrowth Structure Zeolites. *Catalysts*. **2023**, 13(3), 570.
22. Verboekend, D., Mitchell, S., Milina, M., Groen, J.C., Pérez-Ramírez, J. Full Compositional Flexibility in the Preparation of Mesoporous MFI Zeolites by Desilication. *J. Phys. Chem. C*, **2011**, 115, 29, 14193–14203